ELSEVIER

Journal of Crystal Growth 174 (1997) 230–237

JOURNAL OF CRYSTAL GROWTH

Characterization of structural defects in MLEK grown InP single crystals using synchrotron white beam X-ray topography

H. Chung[a,*], W. Si[a], M. Dudley[a], A. Anselmo[b], D.F. Bliss[b], A. Maniatty[c], H. Zhang[d], V. Prasad[d]

[a] Department of Materials Science and Engineering, State University of New York, Stony Brook, New York 11794, USA
[b] US Air Force Rome Laboratory, Hanscom AFB, Massachusetts 01731, USA
[c] Department of Mechanical Engineering, Aero. Eng. & Mech., Rensselaer Polytechnic Institute, Troy, New York 12180, USA
[d] Department of Mechanical Engineering, State University of New York, Stony Brook, New York 11794, USA

Abstract

Structural defects in MLEK grown InP single crystals have been studied using synchrotron white beam X-ray topography. Results here are presented for both a S-doped boule which was wafered longitudinally (i.e., parallel to the growth axis) and an Fe-doped boule which was wafered laterally (i.e., perpendicular to the growth axis). For longitudinal wafers from the S-doped boule, slip bands were observed to have nucleated from high-stress concentration located at the peripheral regions of the boule and to have propagated into the interior of the samples. In the same crystals, the growth interface morphology at different stages of crystal growth was determined. The interface is revealed as contours of equal lattice parameter, visible via strain contrast, as the concentration of the dopant changed periodically during growth. The interface shape was observed to be slightly convex to the melt, once the growth conditions were stabilized. For the laterally sliced wafers from the Fe-doped boule, systematic studies revealed that the density of dislocations changed during growth. A high density of uniformly distributed dislocations were observed in wafers taken from the early and later stages of growth. On the other hand, dislocations in well-defined four-fold symmetric distributions were observed in wafers sliced from the intermediate growth stages. The origins of this four-fold distribution were investigated using a thermal stress model which consisted of imposing a compressive radial stress, uniformly distributed around the boule circumference. The calculated stress distributions also showed four-fold symmetry in agreement with the observed dislocation distributions.

PACS: 61.70.Le; 61.70.Wp; 61.70.Ng

Keywords: X-ray topography; InP; Dislocations and slip bands; Twins; Thermal stresses

1. Introduction

The increasing application of InP crystals as substrates for optical and electronic devices has lead to a heightened demand for the growth of

* Corresponding author. Fax: +1 516 632 8052; e-mail: hchung@ccmail.sunysb.edu.

0022-0248/97/$17.00 Copyright © 1997 Elsevier Science B.V. All rights reserved

PII S0022-0248(96)01110-4

large, high-quality and low-cost single crystals. The growth of InP is complicated by its tendency to deform plastically due to its low-yield stress [1]. In addition, temperature fluctuations imposed by turbulent convective flow can give rise to non-uniform dopant distributions. Therefore, it is important both to suppress turbulent convective flow and to minimize thermal stresses generated during growth processes. Improvements in crystalline quality and dopant distribution uniformity have been demonstrated recently by employing the magnetic liquid encapsulated Kyropoulos (MLEK) method [2]. In this technique, the turbulent convective flow driven by buoyancy and surface tension forces is minimized by the application of an axial magnetic field. In addition, the occurrence of twinning is significantly reduced by using a flat-top shaping technique, avoiding the production of an elongated shoulder region where twins often nucleate.

In this study, defect structures in MLEK grown doped InP crystals have been characterized using synchrotron white beam X-ray topography (SWBXT) [3, 4]. Investigations of structural defect configurations and their distributions in the different stages of crystal growth enabled the determination of the correlation between the development of the defect microstructure and the growth conditions.

2. Experimental procedure

The InP crystals studied were grown at Rome Laboratory, Hanscom AFB, using the MLEK growth method. The details of the growth process and furnace design have been reported elsewhere [2, 5].

SWBXT experiments were carried out at the Stony Brook Synchrotron Topography Station, Beamline X-19C, at the National Synchrotron Light Source (NSLS), Brookhaven National Laboratory. In this study, the transmission Laue geometry is employed. A scanning mechanism [6] comprising both vertical and horizontal translation stages was employed to enable single exposure imaging of large size wafers (1″ × 1″ for Fe-doped wafers and 2.5″ × 1.6″ for S-doped wafers). The crystals were oriented in the beam so that the wavelengths selected for the reflections used were around 0.45 Å, which is just above the In K absorption edge (0.44 Å), to minimize photoelectric absorption. In addition, to prevent possible surface deterioration of the crystals due to prolonged exposure to the intense radiation, the longer wavelength components of the synchrotron radiation, which are most readily absorbed, were selectively removed by employing a filter consisting of a few hundred micrometers of aluminum. All images were recorded on 8″ × 10″ Kodak SR-1 high-resolution X-ray film.

3. Results and discussions

3.1. Fe-doped InP crystals

Systematic imaging of wafers sliced perpendicular to the [0 0 1] growth direction from a Fe-doped InP boule revealed that the density and distribution of dislocations changed at the different stages of crystal growth. Dislocations of very high density were observed in both the initial and final stages of crystal growth, while in the intermediate growth stages, a four-fold symmetric distribution of dislocations was revealed separated by regions of low dislocation density.

Fig. 1 is a transmission X-ray topograph recorded from a wafer sliced near to the seed. A twin lamella (T) nucleated from the flat top of the crystal was observed. Detailed analysis of the diffraction patterns recorded from this twin-related region revealed that the operative twin operation consists of a 180° rotation about the $(1\ 1\ \bar{1})$ plane normal. The X-ray topograph also revealed that a high density of dislocations was generated in this region. The density of dislocations reaches a maximum in the peripheral regions of the wafer along the crystallographic $\langle 1\ 0\ 0 \rangle$ directions. Fig. 2a is a transmission topograph recorded from a wafer sliced from the intermediate growth stages. A well-defined four-fold symmetric distribution of dislocations is evident. The regions of high dislocation density are again observed to lie near the periphery of the wafer along $\langle 1\ 0\ 0 \rangle$ directions, while the density of dislocations reaches a minimum along $\langle 1\ 1\ 0 \rangle$ directions. Fig. 2b is a highly magnified X-ray

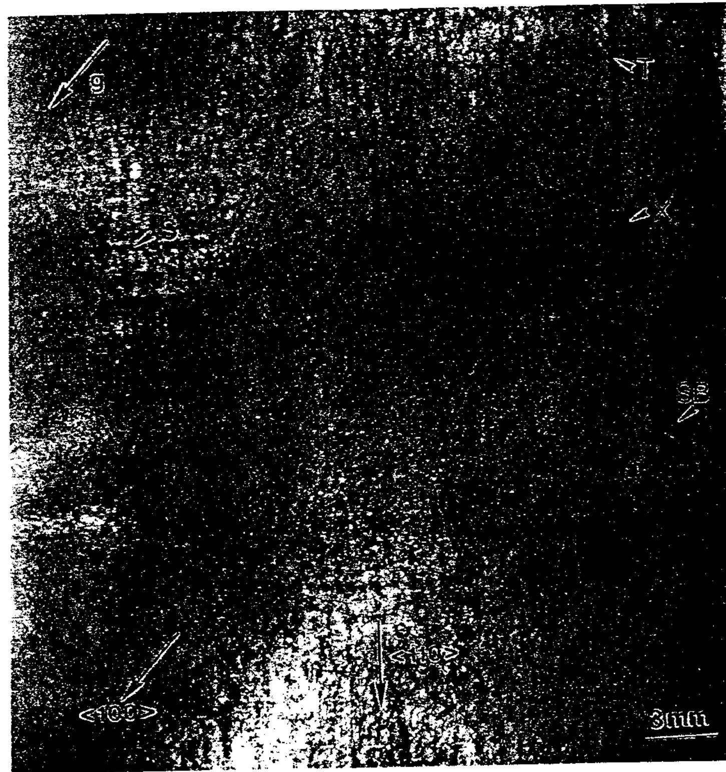

Fig. 1. Synchrotron white beam X-ray topograph ($g = \bar{4}\,0\,0$, $\lambda = 0.45$ Å) recorded from the initial stages of crystal growth showing the formation of a high density of dislocations.

topograph enlarged from region A, where a very low density of dislocations is observed. Individual dislocations (D) are clearly visible. A dislocation density of approximately 10^3 cm^{-2} can be determined. In contrast to Fig. 2b, Fig. 2c is a highly magnified X-ray topograph recorded from region B showing a very high density of dislocations. Since the dislocation density is close to the resolution limit of the technique, a dislocation density of approximately 10^5 cm^{-2} can be deduced from this topograph. Fig. 3 is a transmission X-ray topograph recorded from a wafer sliced near to the tail end of the boule. This topograph revealed a uniformly distributed, high density of dislocations.

X-ray topographic observations revealed that the density and distribution of dislocations changes at the different stages of growth. A high density of dislocations is observed in the region near to the flat top of the crystal where the growth process started. The density of dislocations then decreases toward the intermediate growth stages, and then increases again in the final stages of crystal growth.

3.1.1. Modeling the origin of the dislocation distributions

It has been shown that in liquid encapsulated Czochralski growth, significant radial thermal stresses can be generated when the newly solidified region is pulled from the melt [7]. If the stresses exceed the yield stress of the material, dislocation slip bands can be generated to relieve the excess thermal stresses. The formation of extensive slip bands (S) from peripheral regions in all the wafers studied appears to be consistent with earlier observations. In addition, X-ray topographic studies of dislocation distributions revealed that the density of dislocations changed along different

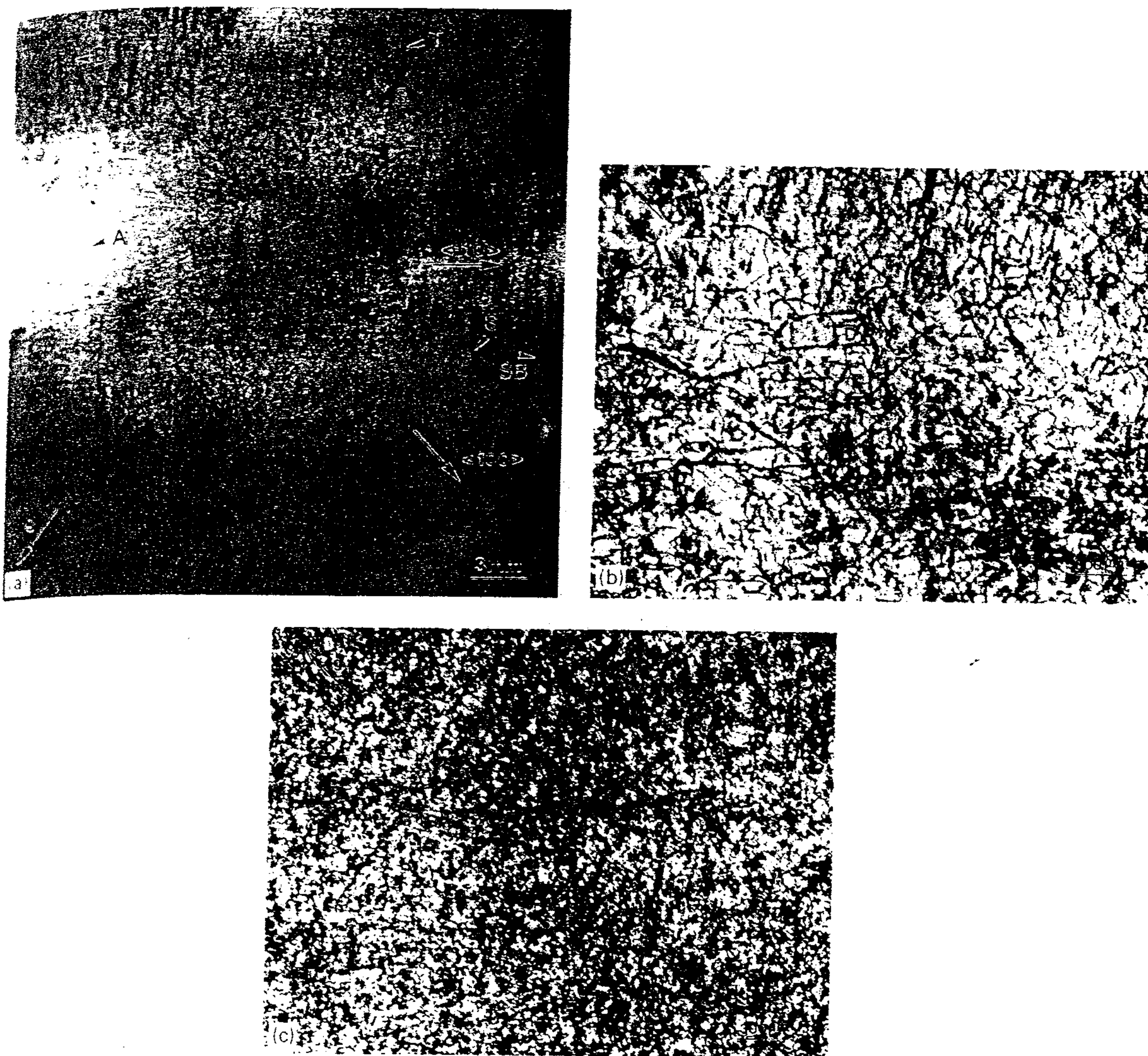

Fig. 2. (a) Synchrotron white beam X-ray topograph ($g = \bar{4}\,0\,0$, $\lambda = 0.45$ Å) recorded from the intermediate stages of crystal growth showing the formation of a four-fold symmetric distribution of dislocations; (b) and (c) are highly magnified X-ray topographs recorded from the regions A and B, respectively.

crystallographic directions. In most of the wafers studied, a high density of dislocations can be observed near the peripheral regions along ⟨1 0 0⟩ directions, while it reached a minimum along ⟨1 1 0⟩ directions. A well-defined four-fold symmetric distribution of dislocations was also observed in wafers sliced from the intermediate growth stages. In order to investigate the origin of such dislocation distributions, a thermal stress model composed of uniformly distributed, compressive radial stress was introduced.

Slip in crystals with the zinc blende structure such as InP are activated on twelve {1 1 1}⟨1 1 0⟩ slip systems. The resolved shear stress for each of these slip systems for crystals grown along the [0 0 1] direction can be calculated using Schmid's law [8]. Fig. 4 shows the calculated shear stress distribution on the (0 0 1) plane. The shear stress

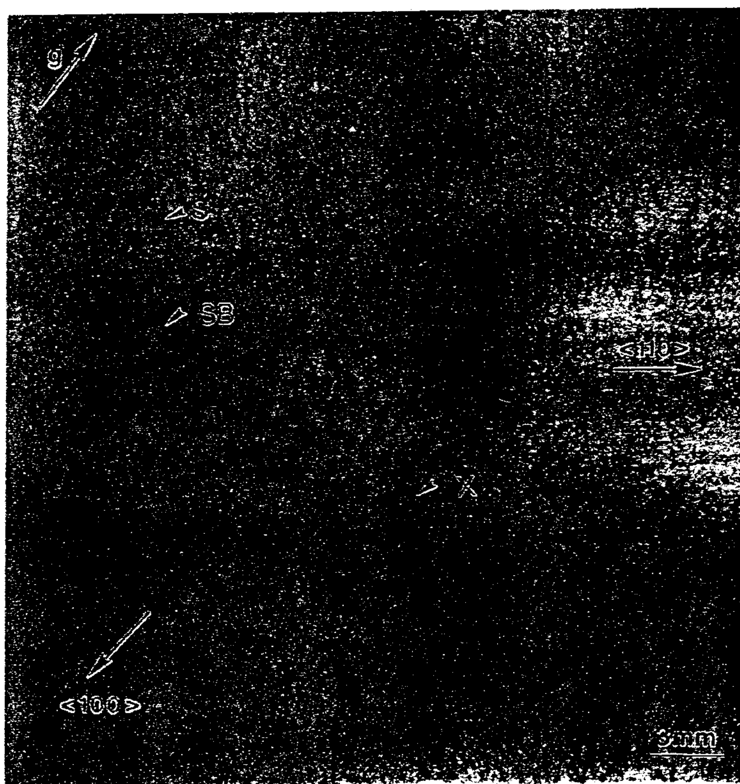

Fig. 3. Synchrotron white beam X-ray topograph ($g = 4\ 0\ 0$, $\lambda = 0.45$ Å) recorded from the final stages of crystal growth showing the formation of a high density of dislocations.

reached its maximum along the crystallographic ⟨1 0 0⟩ directions, while it reached a minimum along the ⟨1 1 0⟩ directions. Since the overall dislocation density is proportional to the total excess shear stress, which in turn is related to the local shear stress value, the calculated result is in good accord with the observed dislocation distributions. It is, therefore, expected that the compressive radial shear stresses likely to be experienced by the crystal during growth can give rise to dislocation generation which leads to the observed distribution.

3.2. S-doped InP crystals

3.2.1. The morphology of growth interfaces

In melt growth, the morphology of the growth interface is strongly influenced by the growth conditions. Important information regarding the temperature profile of the melt, microscopic growth rate variations and the relationship between growth conditions and crystal perfection can be directly deduced through the observation of the shape of the growth interface at the various stages of growth. In both LEC and LEK growth methods, growth rate fluctuations caused by effects such as unstable thermal convection and crystal rotation can give rise to inhomogeneous dopant segregation along the instantaneous solid–liquid interface [7, 9]. Precipitation of the dopant material can occur if the dopant concentration reaches its solubility limit. This leads to a lattice distortion (mainly a lattice parameter variation) along the solid–liquid interface. If the lattice distortion creates a local misorientation which is greater than the perfect crystal rocking curve width, growth striations can be revealed on X-ray topographs as contours of equal lattice parameter [10]. The high degree of strain sensitivity ($\Delta d/d \sim 10^{-5}$–10^{-8}) of X-ray topography

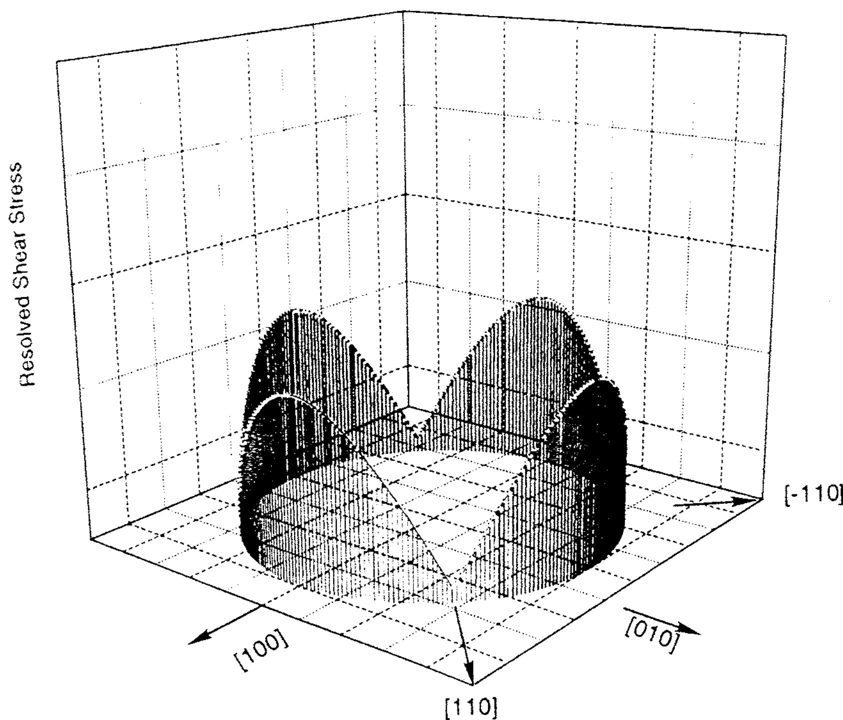

Fig. 4. The distribution of resolved shear stresses on a plane perpendicular to the (0 0 1) growth direction in crystals subjected to thermal-gradient-induced, uniformly distributed, compressive radial stresses.

is particularly well suited for detecting the small strains associated with the small changes in dopant concentration. Thus, the shape of the solid–liquid interface at various stages of growth can be determined through the observation of these striations.

Fig. 5 is a transmission X-ray topograph recorded from a (1 1 0) wafer sliced longitudinally from a heavily sulfur-doped [0 0 1] InP crystal. The morphology of the growth interface at the different stages of crystal growth is clearly delineated by the growth striations (GS). In the initial growth period, when the flat top of the crystal was grown, no pulling was employed. A growth interface convex to the melt was observed. However, a significant change in growth interface morphology occurred when the pulling process was initiated. A bimodal shape of growth interface, comprising a convex region in the center and two concave regions near the outer surface of the crystal was developed. In the MLEK growth method, the axial temperature gradient in the melt is low (20–40°C/cm) so that a small temperature fluctuation can influence the stability of crystal growth [2]. An abrupt change in the morphology of the growth interface indicates the occurrence of a significant temperature fluctuation when the pulling process started. This can possibly upset the stability of the crystal growth and lead to dislocation generation.

X-ray topographic observations also clearly revealed the evolution of growth interface morphology in the subsequent stages of crystal growth. For the outer surface region, the curvature of the concave interface decreased gradually, while the concave growth front moved into the interior of the crystal. On the other hand, the curvature of the concave growth interface decreased. This result strongly indicated that the temperature fluctuation generated in the beginning of the pulling process can have an effect on the stability of the growth conditions in the later stages of crystal growth, while the decrease in the curvature of the concave interface suggested the suppression of temperature

Fig. 5. Synchrotron white beam X-ray topograph ($g = 0\,0\,4$, $\lambda = 0.45$ Å) recorded from a longitudinal cut (1 1 0) S-doped InP wafer showing the morphology of the growth interface (I) and the formation of slip bands (S_1 to S_3).

fluctuations in the following stages of crystal growth. A well defined, slightly convex shape of growth interface was developed in the final stage of crystal growth. The temperature fluctuation generated at the beginning of the pulling process has, by this point, fully diminished. The recovery of growth interface morphology strongly suggests that the thermal and growth conditions in the subsequent growth stages were stabilized so that no new, significant temperature fluctuations disturbing the growth interface after the pulling process started were experienced.

3.2.2. The distribution of dislocations

In melt growth, dislocations can be generated during crystal growth if growth accidents such as large temperature fluctuations and compositional inhomogeneity occur [7]. On the other hand, dislocation multiplication and propagation can occur if thermal stresses were introduced during the cooling process. Investigations of the distribution and configuration of dislocations are important to determine the relationship between dislocation generation and the growth conditions used.

A very high density of dislocations was observed in the region where the significant changes occurred in the morphology of the growth interface. The variation in the morphology of the growth interface evidenced the instability of the growth conditions. It is expected that large thermal stresses can be induced by temperature fluctuations and give rise to the formation of a high density of dislocations observed in this region. In addition, numerous slip bands (S_1 to S_3) nucleated from the peripheral regions and propagating into the interior of the crystal were also observed. The diffuse contrast in the slip bands and in their surrounding crystal volume is due to the long-range strains associated with a high density of dislocations piling up on their slip planes [11, 12]. By analyzing the projected direction of these slip bands in different reflections, they were determined to be lying on the $(1\,1\,\bar{1})$, $(1\,\bar{1}\,1)$, and $(\bar{1}\,1\,1)$ planes, respectively. In the crystal studied, dislocations were caused by plastic deformation to relieve excessive thermal stresses associated with large temperature gradients developed during the pulling and the subsequent cooling processes. This result strongly indicated that an optimization of the thermal conditions during crystal growth can be important to improve the crystalline perfection in as-grown crystals.

4. Conclusions

4.1. Fe-doped InP crystal

1. A thin twin lamella nucleated from the flat top of the boule, where the growth process initiated, is observed. The twinning operation is determined to be a 180° rotation about the (1 1 $\bar{1}$) lattice plane.

2. The density and distribution of dislocations changed in the different stages of crystal growth. A very high density of dislocations was generated in both the initial and final stages of crystal growth, while a well-defined four-fold symmetric distribution of dislocations is observed in the intermediate growth stages.

3. The distribution of shear stresses in a plane perpendicular to the [0 0 1] growth direction is calculated using a thermal stress model which involved the application of a uniformly distributed, compressive radial shear stress. The calculated result is in good agreement with the observed dislocation distributions.

4.2. S-doped InP crystal

4. The morphology of growth interfaces can be strongly influenced by the growth conditions. A significant change in growth interface morphology occurred when the pulling process was initiated. The likely origin for this lies in the fact that the global heat transfer environment of the growth process, which includes both the convection flow driven by buoyancy and surface tension and the thickness of the encapsulant layer, were changed when the pulling process started. This can potentially cause a change of the flow pattern of the melt and give rise to a modification of the growth interface morphology. In the crystal studied, a bimodal shape of growth interface comprised of a convex interface in the center and two concave components near the outer surfaces of the crystal was developed.

5. Numerous slip bands nucleated from peripheral regions and propagating into the interior of the crystal were observed. This observation revealed that thermal stresses associated with large temperature gradients were induced during the pulling and the subsequent cooling processes. It is expected that an optimization of the thermal conditions during crystal growth can significantly improve the crystalline perfection in as-grown crystals.

Acknowledgements

The work was supported by ARPA/AFOSR consortium of crystal growth research under the contract F496209510407. Topography was carried out at the Stony Brook Synchrotron Topography Facility, beamline X-19C, at the National Synchrotron Light Source, at Brook National Laboratory, which is supported by the Department of Energy.

References

[1] M. Azzaz, J. Michel and A. George, Phil. Mag. A 69 (1994) 903.
[2] D.F. Bliss, R.M. Hilton and J.A. Adamski, J. Crystal Growth 128 (1993) 451.
[3] M. Dudley, in: Applications of Synchrotron Radiation Techniques to Materials Science, Eds. D.L. Perry, R.L. Stockbauer, N.D. Shinn, K.L. D'Amico and L.J. Terminello, Mater. Res. Soc. Symp. Proc., Vol. 307, Pittsburgh PA (1993) p. 213.
[4] M. Dudley, in: Encyclopedia of Advanced Materials, Vol. 4, Eds. D. Bloor, R.J. Brook, M.C. Flemings and S. Mahajan (Pergamon, Oxford, 1994) p. 2950.
[5] V. Prasad, D.F. Bliss and J.A. Adamski, J. Crystal Growth 142 (1994) 21.
[6] S. Wang, M. Dudley, W. Huang, C.H. Carter, Jr., V.F. Tsvetkov and C. Fazi, in: Semiconductor Characterization Present Status and Future Needs, Eds. W.M. Bullis, D.G. Seiler and A.C. Diebold (AIP, New York, 1996) p. 278.
[7] D.T.J. Hurle and B. Cockayne, in: Characterization of Crystal Growth Defects by X-Ray Methods, Eds. B.K. Tanner and D.K. Bowen (Plenum, New York, 1980) p. 46.
[8] E. Schmid and W. Boas, Plasticity of Crystals (Chapman and Hall, London, 1968).
[9] J.R. Carruthers and A.F. Witt, in: Crystal Growth and Characterization, Eds. R. Ueda and J.B. Mullin (North-Holland, Amsterdam, 1975) p. 107.
[10] B.K. Tanner, X-Ray Diffraction Topography (Pergamon, Oxford, 1976).
[11] A. Authier and A.R. Lang, J. Appl. Phys. 35 (1964) 1956.
[12] J. Wu, T. Fanning, M. Dudley, V. Shastry and P. Anderson, in: Defect Engineering in Semiconductor Growth, Processing and Device Technology, Eds. S. Ashok, J. Chevallier, K. Sumino and E. Weber, Mater. Res. Soc. Symp. Proc., Vol. 262, Pittsburgh PA (1993) p. 265.